
# Benchmarking a quasi-steady method for predicting propeller unsteady loads

**Richard Howell (1,2), Paul Dylejko (1), Paul Croaker (1,3) and Alex Skvortsov (1)**

(1) Maritime Division, Defence Science and Technology, Melbourne, VIC 3207, Australia
(2) YTEK Pty Ltd, Level 1, 231 High St, Ashburton, VIC 3147, Australia
(3) School of Mechanical and Manufacturing Engineering, UNSW, Sydney NSW 2052, Australia

## ABSTRACT

Aircraft and ships suffer from unwanted noise and vibration due to propeller unsteady loads. When trying to achieve low levels of propeller noise and vibration during design, the designer must balance these against often conflicting goals such as required thrust and fatigue strength. During trade-off studies, there is value in having a range of validated modelling tools that can be used over a range of timescales with different levels of fidelity. Simplified physics-based models are often useful because they allow for a large investigation of the parameter design-space and they can also provide insights into what are the most important in-flow characteristics and design parameters. This paper brings together a range of simplified techniques that assume a quasi-steady state, to assess the tonal unsteady propeller loads resulting from an ingested non-uniform wake. As a first step in validating this approach, predicted results are compared against previously published experimental measurements of two model propellers at the David Taylor Research Centre (DTRC). Results show that under the right conditions, this approach can give good predictions. The instances where the methodology does not predict the response well are also demonstrated.

## 1 INTRODUCTION

Marine propellers operate in unsteady, spatially non-uniform flow which is formed by merging the turbulent boundary layer and the wake from the hull of a ship. As the propeller rotates, the blades interact with this non-uniform flow and develop unsteady periodic loads. Assuming a linear response, these periodic thrust and torque harmonics result from inflow wake harmonics that match multiples of the number of blades, N.B. The transverse force is associated with $\pm 1$ blade harmonics. Quasi-steady (QS) methods allow quick assessment of propeller unsteady forces from changes in wake harmonics. More accurate but slower models in order of increasing accuracy and computational cost include: lifting-line theory, the boundary-element method (BEM), Unsteady Reynolds Averaged Navier-Stokes (URANS) and Large Eddy Simulation. The purpose of this paper is to summarise what is currently known on this topic in the available literature and to benchmark application of the QS method to current hydrodynamic propeller problems. This work complements that of Jin et al. (2018) who developed a BEM model of this problem.

The investigation of propeller unsteady response to a non-uniform wake has been a focus of research for many years. Early numerical studies relied upon the use of the QS method to compare with experimental results owing to minimal computational resources available e.g. see McCarthy (1961). To generate unsteady load predictions, the QS method relies upon experimental data of the flow field in which the propeller is operating: this flow field is termed an ‘effective wake’. This data is challenging to measure and so an alternate method is to use data from ‘nominal wakes’: this is the wake generated by a ship if it were to be towed in the absence of a propeller. Clearly, the nominal wake data will not capture the coupled fluid-structure interaction between the propeller, the flow and the body of the ship. Fundamental studies that seek to benchmark methods for estimating unsteady load use nominal wake data generated by a wake screen; a 3-cycle wake screen is shown at the top of Figure 1 from Jessup (1990). Boswell and Miller (1968) obtained accurate, fundamental experimental-measurements of nominal wakes using three and four cycle screens; Jessup (1990) extended these fundamental results using six, nine and twelve cycle screens. The unsteady load measurements of Jessup (1990) are used below to quantita-

tively validate our QS method for prediction of propeller unsteady loads. The application of the QS method to propellers in general is then discussed and finally extensions of the QS methods are introduced.

## 2 METHOD

### 2.1 Nominal Wake & Propeller Properties

Jessup (1990) obtained detailed nominal wakes behind 3, 6, 9 and 12 cycle wake screens. Measurements of the nominal wake velocity signal between $0$ and $2\pi$ rad at four different radial locations ($0.3\mathrm{R}$, $0.5\mathrm{R}$, $0.7\mathrm{R}$ and $0.9\mathrm{R}$ where $\mathrm{R}$ is the propeller radius) were taken via a pitot tube. The first $q = 15$ harmonics of the Fourier series of these signals were tabulated. The velocity signals can be reconstructed from the Fourier series data by using the formulae

$$V_x(r,\theta)/V_{\mathrm{VM}}(\theta) = \sum_{q=1}^{15}\left(A_q(r)\cos q\theta + B_q(r)\sin q\theta\right) = \sum_{q=1}^{15}\left(C_q\cos\left(q\theta - \phi_q\right)\right), \quad (1a,b)$$

where $V_x$, $\theta$, $A_q$, $B_q$, $C_q$ and $\phi_q$ are respectively the axial flow velocity, angular coordinate of wake velocity, cosine and sine coefficients of the Fourier series and the phase of these coefficients. The value $V_{\mathrm{VM}}$ is the spanwise, volumetric-mean velocity and is calculated as

$$V_{\mathrm{VM}}(\theta) = \frac{2}{R^2 - r_h^2}\int_{r_h}^{R} V_x(r,\theta)rdr\,, \quad (2)$$

where $r_h$ is the propeller hub radius. As an example, the reconstructed wake properties for the 3-cycle screen are shown in the bottom of Figure 1.

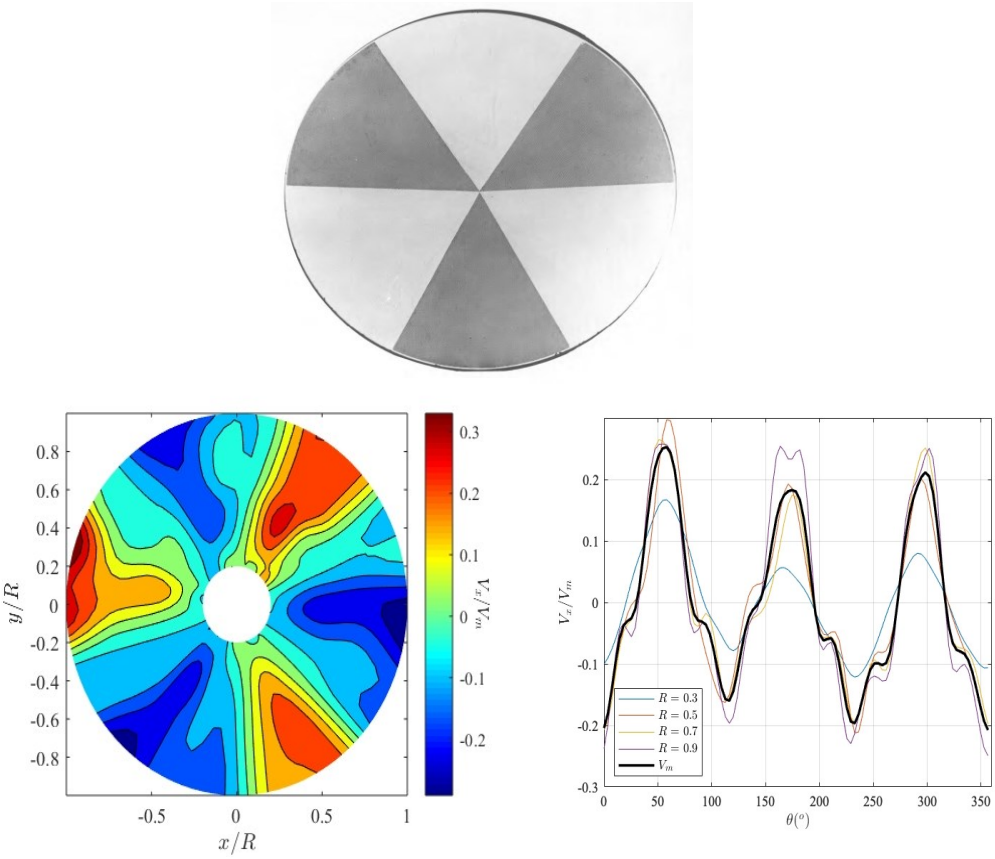


Source data: Jessup (1990).

Figure 1. Top: 3 cycle wake screen, Bottom: reconstruction of wake velocities.

The propellers studied herein are NSRDC Propellers 4119 and 4132 that both have a Blade Number $B = 3$, diameter $D = 0.306$ m and expanded area ratios (EAR) of 0.6 and 0.3 respectively: these are shown on the left-hand side of Figure 2; on the right–hand side, their 'open water' characteristic curves are shown that detail propeller performance for a uniform inflow. The properties plotted are the variation in non-dimensional thrust $K_T = T/(n^2D^4)$, torque $K_Q = Q/(n^2D^5)$ and efficiency $\eta = (K_T/K_Q)(J/2\pi)$ with Advance Coefficient $J = V/nD$ where $V$ is the representative velocity and $n$ is the number of revolutions per second (Full explanation of these terms are given in numerous marine propulsion text books, e.g. Carlton (2012)). Herein, the propellers both have an operating advance coefficient of $J_0 = 0.833$. The propeller blade cross-sections are modified NACA 66 aerofoils with zero skew and rake. From Smith & Slater (1988), blade skew moves a section of the blade around the shaft axis in the flow direction, opposite to the direction of shaft rotation; it is applied to reduce the unsteady hydrodynamic loading on the blade when the propeller is operating in a highly non-uniform wake behind the ship's hull. Rake is an aft or forward displacement of the blade section and is used to increase clearance between the hull and propeller.

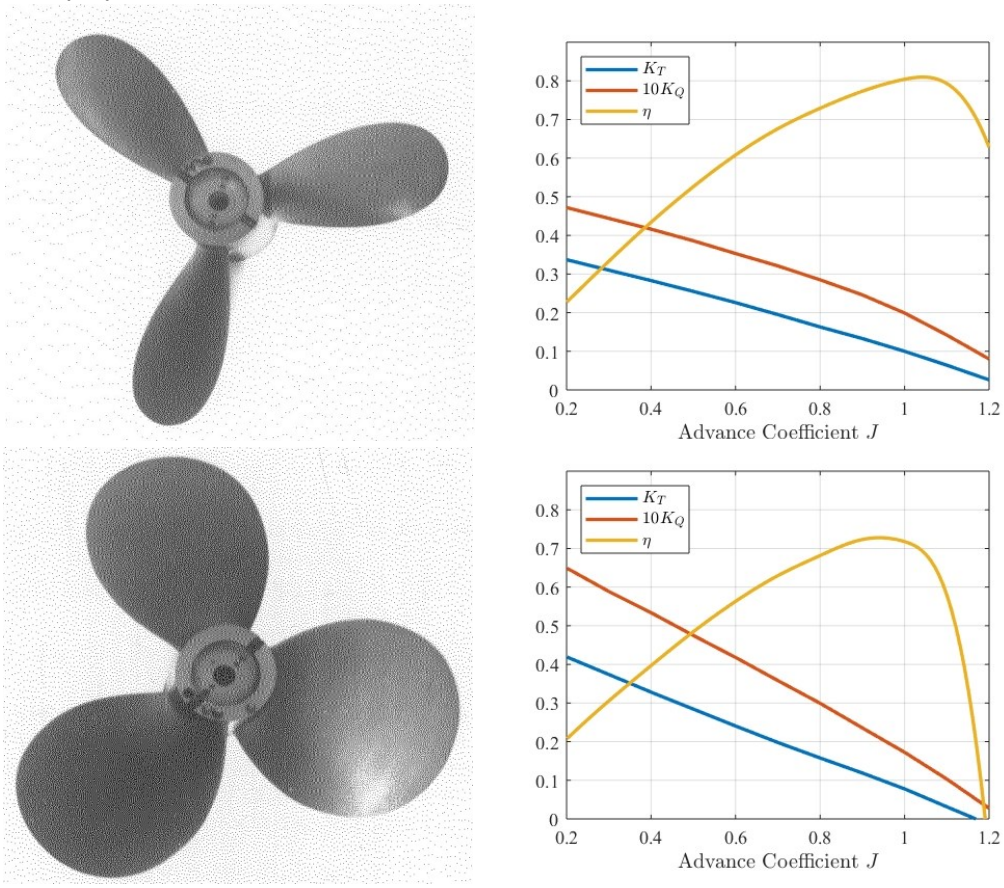


Source data: Denny (1968), Boswell & Miller (1968), Kerwin (1976).
Figure 2: DTRC Propellers 4132 (top) and 4119 (bottom) and their open water performance characteristic.

### 2.2 The Quasi-Steady (QS) Method

To obtain an estimate of unsteady thrust, the QS method combines open propeller characteristic curves with nominal wake data; for an early example see McCarthy (1961). A prediction of the unsteady thrust is obtained by 'oscillating' about $J_0$ on the thrust curve: for each harmonic the unsteady thrust is

$$K_{Tq} = \frac{\Delta K_T}{\Delta J}\frac{\Delta J}{J}J \quad \text{where} \quad \frac{\Delta J}{J} = \frac{\Delta V}{V'} - \frac{\Delta n}{n'} \quad \textbf{or} \quad \frac{\Delta J}{J} = \frac{V + V_x(r,\theta)}{(\Delta n/n')D} \quad \text{where} \quad \frac{\Delta n}{n'} = \left(1 + \frac{V_\theta(r,\theta)}{2\pi qr}\right), \qquad \text{(3a,b,c,d)}$$

the presented methods from Sasajima (1978) (Eqn. (3a,b)) and Tanibayashi (1980) (Eqns. (3a,c,d)), the latter method requiring wake tangential velocity data, $V_\theta$. Both these techniques combine information from the open water propeller characteristics with the velocity data obtained from the nominal wake using Eqns. (1) and (2).

As described in Kerwin (1986), the unsteady problem is complicated by the presence of shed vorticity in the wake that depends on the past history of the circulation around the blades. The non-dimensional parameter that characterizes the degree of unsteadiness of the flow is the reduced frequency $\kappa_1$, a non-dimensional wave number, which is defined as the number of wavelengths per half chord; this can be equated as the product of the frequency of encounter and the local semi-chord, divided by the relative inflow speed

$$\kappa_1 = \frac{\omega}{U}\frac{c}{2} = \frac{\pi c}{\lambda} = \frac{q}{r}\frac{c}{2}, \qquad \text{(4a,b,c)}$$

where $\omega$ and $U$ are the incident frequency and speed respectively and $c$ is chord length of the propeller. The second form Eqn. (4b) is a ratio of the two length scales of the flow field (Boswell & Miller, 1968) where $\lambda$ is the incident wavelength. The third form is the wave number non-dimensionalised by the semi-chord. Clearly, the chord length varies with radius: in general the most heavily loaded area of the propeller is at $r \approx 0.7R$, which leads to a simplification from Roddy (2011) to allow estimation of $\kappa_1$ as $2.74\ \mathrm{EAR}$. This value is for a single blade: for a multi-bladed propeller the reduced frequency is multiples of the ratio of harmonic number to blade number i.e. $q/B$. For large $\lambda$ the unsteady lift is equal to the 2D quasi-steady lift approximation. As $\lambda$ reduces, the lift reduces owing to unsteady effects: this reduction can be approximated by various functions for different physical situations and some of these are plotted in Figure 3. Of major importance is the factor $|S(\kappa_1)|$ or Sear's function, which gives a baseline conservative estimate of the reduction in lift owing to unsteady effects, e.g. see Glegg & Devenport (2017); also of importance for the current research is the factor $|f_3(\kappa_1)|$ published by Sasajima (1978). These two factors are equated as

$$|S(\kappa_1)| = \frac{2}{\pi\kappa_1\left(H_0^{(1)}(\kappa_1) + iH_1^{(1)}(\kappa_1)\right)} \qquad \text{and} \qquad |f_3(\kappa_1)| = \left(J_0^{(1)}(\kappa_1)^2 + J_1^{(1)}(\kappa_1)^2\right)^{0.5}, \qquad \text{(5a,b)}$$

where $H$ and $J$ are Henkel functions and Bessel functions respectively, both of the first kind. These factors are used to multiply and hence reduce the predicted values of unsteady thrust to account for the unsteady lift; the $f_3$ correction improves the Sear's function for the current research focus as it uses a distributed load along the chord length rather than using a point force. Breslin (1970) states that the QS method is generally applicable at low values of Mach number and $\kappa_1$ which is generally the case when modelling marine propellers.

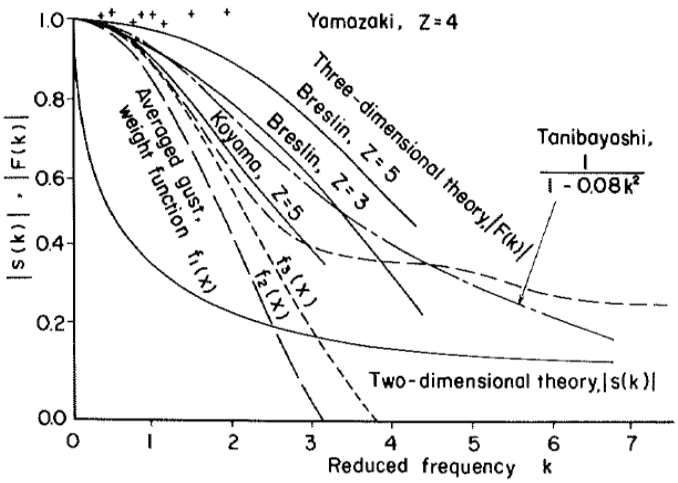


Source: Sasajima (1978).
Figure 3: Unsteady lift correction function variation with reduced frequency.

## 3 RESULTS

### 3.1 Comparison with Experiment

Kerwin (1986) states that with the onset flow represented in terms of its circumferential harmonic components, and with the assumption that the propeller responds linearly to changes in the onset flow, the problem of calculating the unsteady thrust of a propeller can be reduced to one of finding the response of the propeller to each harmonic. Figure 4 plots the trend of the 'principle harmonics' of the unsteady thrust for each of the four wake screens, e.g. the 3rd harmonic in the 3 cycle wake, the 6th harmonic in the 6 cycle wake and so on; the left and right figures are for propellers 4132 and 4119 respectively. The experimental data of Jessup (1990) are denoted by the 'o' markers; the error bars show the relative experimental error and are discussed in more detail in Section 3.2 below. Jessup (1990) also produced numerical predictions from their unsteady lifting surface theory code PUF-2 and these are joined by the dotted line. The graphs confirm the trends shown in Figure 3 that as the wake becomes more complex and frequency rises, the unsteady thrust of the propeller drops. For propeller 4132 the results of the QS method using the $f_3$ correction (dashed line) compare well with the experimental data and the PUF-2 model and they are of comparable accuracy to those obtained by Jin et al. (2018) who used BEM and URANS models. The QS method without an unsteady correction (+ markers) gives a realistic upper bound (over-estimation) of the unsteady thrust likely to be produced by a propeller, whilst with the Sears correction of Eqn. (5a) (x markers) gives a realistic lower bound (under estimation). Less accurate agreement is found for propeller 4119 which has higher EAR. Breslin & Henderson (1996) concluded that QS methods lose accuracy modelling wider propeller blades because the lift slope is too high and unsteady reductions are too large. The discrepancy occurs for the larger harmonics, and hence higher reduced frequencies; however, the lower bound of the experimental results is still captured by the conservative estimate of the Sear's corrected prediction and is within experimental error bounds.

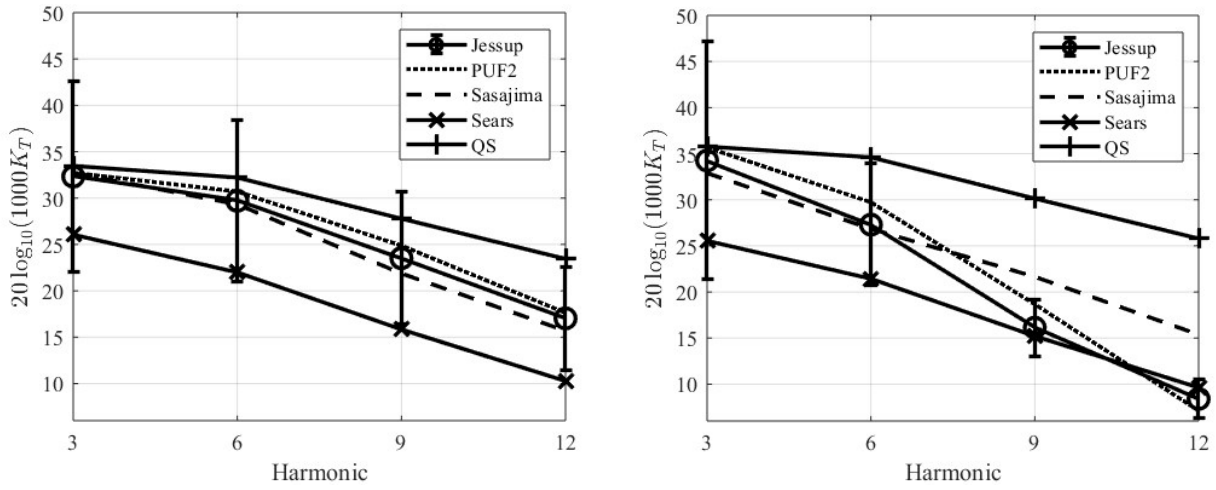


Figure 4: Comparison of Unsteady thrust calculation methods: Left: Propeller 4132, Right: Propeller 4119.

### 3.2 General Application of the QS method

Although the QS method works well for the data provided by Jessup (1990), what confidence do we have that the curves plotted in Figure 4 are universal? That is, will the QS method work for other data, such as in the wake of a ship in a heavy sea? Modern propellers are to be made of composites so we would like to include blade flexibility effects e.g. see Maljaars et al. (2018). Is the model robust enough to include this? By identifying where the QS method loses accuracy we can address whether this can be remedied: this will then inform us on how to design future experiments and numerical studies.

Kerwin (1986) examines several issues on this topic: First, he states that it is not clear how much the harmonic content of the effective wake field differs from that of the nominal wake behind a maritime vessel, although it is possible that a pure single harmonic wake generated by a screen in a water tunnel will not be altered appreciably by the induced velocity field of the propeller. Second, Kerwin then describes how a number of semi-empirical methods were applied to a specific case in an international cooperative study conducted by Schwanecke (1975); the study showed that a large spread existed in the results obtained by the different methods. Lastly, Kerwin describes how unsteady propeller force measurements are extremely difficult to make, since the propel-

ler shaft and measuring system must be carefully designed and dynamically calibrated, and the resulting output signals must be processed to remove noise, a problem made even more complicated as the unsteady thrust and velocity variations are relatively very small values compared to the steady thrust and in-flow velocity. In Figure 4, the relative error bars are shown for the experimental data: this error is detailed in Jessup (1990) for the measurements of rpm, thrust and velocity. Overall, the major source of error is from the velocity measurement, except for the higher order wake screen modes where the relative error of measurement of unsteady thrust of 'non-principal harmonics' (i.e. thrust harmonics that are not equal to the cycle number of the wake screen) is very large as the magnitude measured is very small. The message here is that more confidence can be had in the results of the QS method if there is confidence in the quality of the experimental data utilised.

A further weakness of the QS method is described by Breslin (1970) who states that it will not work when the wake properties have a phase change in the spanwise (radial) direction. It should be noted that propeller suction will add further spanwise effects (magnitude but not phase). To investigate the current nominal wake data in this respect, Figure 5 plots the magnitude and phase ($C_q$ and $\phi_q$ from Eqn. (1)) of the harmonics of wake axial velocity at different values of radius. The top row show the magnitudes and that the principle harmonic generally gives a strong signal; however, the bottom row shows the phase and that although the principal mode is almost always of the same phase, the non-principal harmonics almost always change phase over the radius.

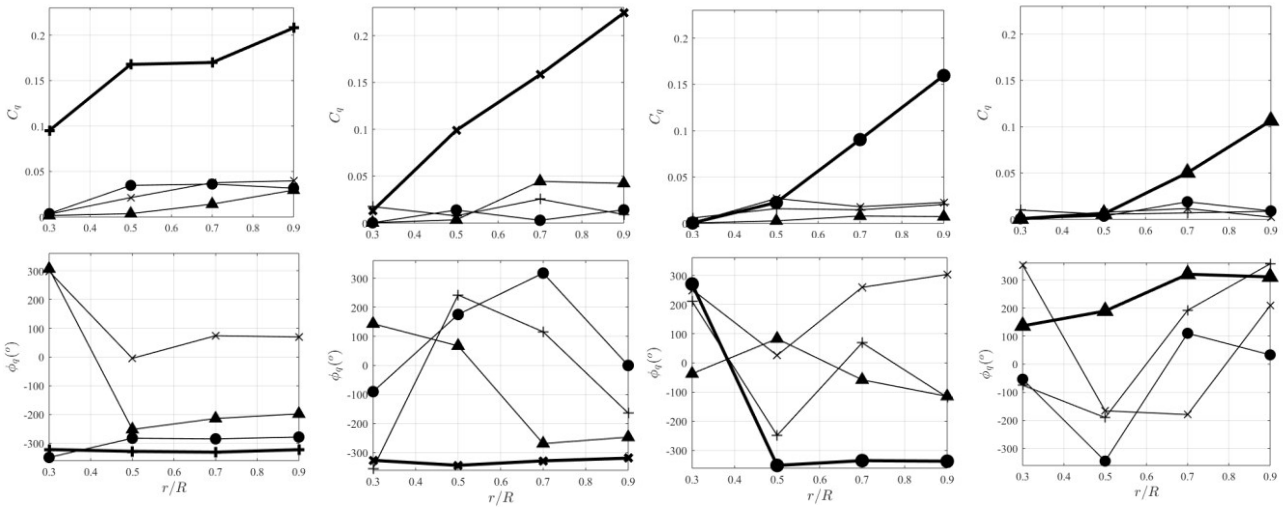


Source data: Jessup (1990).

Figure 5: Properties of harmonics of axial velocity of effective wake along radius (spanwise) for (left to right) 3, 6, 9 and 12 cycle wakes. Upper row: Amplitude, Lower row: Phase. Harmonics: + 3, × 6, ● 9 and ▲ 12. The principal mode in each figure is highlighted by a thicker line type.

This phase change owes to three-dimensional effects, in particular they can be represented as 'obliqueness' in spanwise gust incidence, where the 'oblique angle' $\beta$ is the angle between the gust direction and the blade vertical axis. This topic has been well studied and remains of current interest e.g. see Kazarina & Golubev (2019). A further improvement to the unsteady lift corrections of Eqns. (5a,b) can be implemented by using a correction factor that incorporates the oblique angle: similarly to the functions plotted in Figure 3, this factor reduces in magnitude less than one the greater the obliqueness present in the gust wavefront. Herein, we implement the method of Mugridge (1970) who calculated the reduction in unsteady lift owing to an oblique gust along an aerofoil as

$$T(\kappa_1,\beta) = \frac{\kappa_1^2 + 2/\pi^2}{\kappa_1^2 + (2/\pi^2) + (\kappa_1/\tan\beta)^2} \quad \text{where} \quad \tan\beta = \frac{q}{r}\frac{dr}{d\phi}\,, \tag{6a,b}$$

where the value of $\beta$ can be calculated from the phase information shown in the bottom row of Figure 5 at $0.7R$.

To see if any improvement is made, we now use 'non-principal harmonics' from the experimental data so that, for example, when data from higher order nominal wakes do not exist, we can still predict the unsteady thrust accurately for higher order modes. These are plotted in the form of the 'transfer function': this is equated as the unsteady thrust divided by the volumetric-mean velocity and gives a relative measure of how energy from the

mean flow is being converted into thrust by each harmonic. The transfer function is plotted in Figure 6 using the Jessup (1990) experimental data: the principal harmonics are denoted by the 'o' markers, the data solely from the 3 cycle wake screen by the dashed line and the latter corrected for obliqueness by the dotted lines. When implemented, relative to the prediction of the 3 cycle wake screen, at worst the correction provides no improvement but at best provides a moderate increase in accuracy, the greatest improvement for the 6th harmonic for the larger EAR propeller.

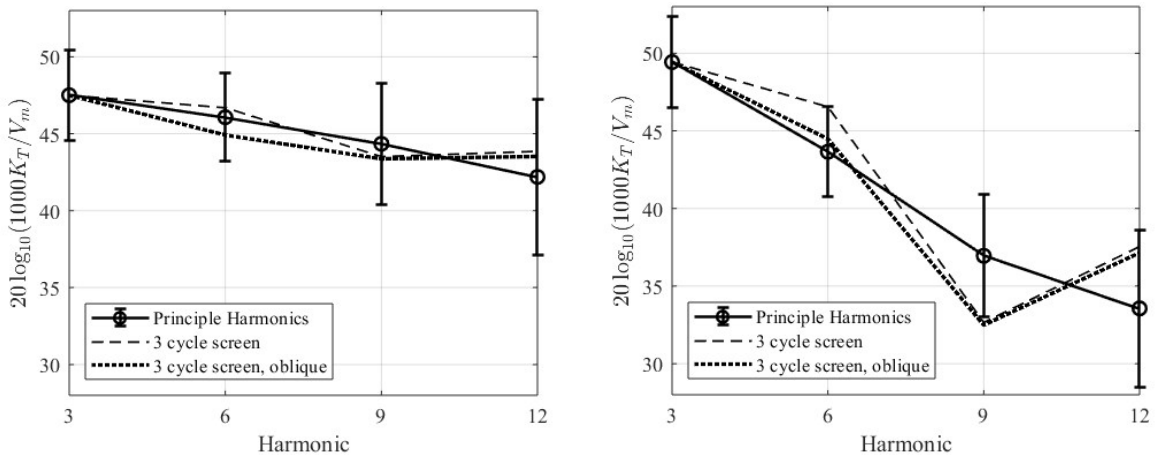


Adapted from Jessup (1990).

Figure 6: Comparison of Unsteady thrust calculation methods. Left: Propeller 4132, Right: Propeller 4119.

### 3.3 Extensions of the QS Method

The QS model can be readily extended to include useful variations and here we describe three such extensions:

**i) Semi-empirical model:** if the open water performance curve (see right-side of Figure 2) for a propeller is not available, it can be estimated using a semi-empirical model. For example, a generic prediction of $K_T$ detailed in Blake (2017) is

$$\frac{K_T}{EAR}\left(1+\frac{3\pi EAR}{B}\right) \approx \frac{\pi^3}{24}\frac{\left(1+(J^2/\pi^2)\right)}{(1+(J/0.7\pi)^2)}\{C_L+(2\pi/0.7\pi)[(P/D)-J]\}\cos\left(\frac{J+P/D}{0.7\pi}\right)I_a \ , \tag{7}$$

where $\mathrm{P/D}$ is the pitch diameter ratio at $0.7\mathrm{R}$ and $C_L$ is the 2-D coefficient of lift of the propeller cross-section at zero angle of attack; herein $\mathrm{P/D}$ has a value of 1.1 (Boswell & Miller, 1968) and $C_L = 0.1355$ for a NACA 66 at a Reynolds Number $\mathrm{Re} \approx 4\times10^5$ based on tip speed. The term $I_a$ is a measure of 'blade interference', a reduction in thrust owing to how much the propeller blades overlap and only has a value less than 1 for $\mathrm{EAR} > 0.3$; from Blake (2017), $I_a = 0.85$ for $\mathrm{EAR} = 0.6$.

**ii) Effective angle of attack:** it is possible to use the QS method to estimate the unsteady forces by recasting the axial and tangential harmonic content of a wake into a change in effective angle of attack $\alpha_{\mathrm{nom}}$ at $0.7R$. For example, interpolating the values of $\alpha_{\mathrm{nom}}$ for the qth harmonic over the blade radius and extracting the value at $0.7R$ allows the calculation of the change in thrust as

$$dJ \ = \ \pi\tan(\gamma+\alpha_{\mathrm{nom}}) - J_0 \qquad \text{where} \qquad \gamma = \tan^{-1}(V_{\mathrm{x}}/V_{\theta}) \ , \tag{8a,b}$$

where $\gamma$ is the hydrodynamic pitch angle. Inserting $dJ$ into Eqn. (3a) allows determination of the unsteady thrust of the propeller of the principal harmonic.

**iii) Blade Skew:** the effect of blade skew can be captured by considering an effective line of encounter, which is implemented by phase shifting the value of $\theta$ in Eqn. (1) by the angle of skew of the propeller. The introduction of skew will lead to further oblique effects that require calculation in a similar way to that described in Eqn. (6) e.g. see Blake (2017).

### 3.4 Future Work

Future work will continue to look for low computational cost, generalised methods that can characterise how changes in a nominal wake will affect propeller unsteady thrust, not necessarily using the QS method. For ex-

ample, Breslin (1971) provides an alternate methodology that calculates transfer functions at multiple radial locations which promises to capture more detail of the flow characteristics. Additionally, more refined experimental data of nominal wakes would be of use to further investigate the validity of the spanwise corrections using Eqn. (6a) e.g. Valentine & Kader (1976). This experimental data could also be replicated numerically, a task that is still beyond the capability of Direct Numerical Simulation at the Reynolds number required, so high fidelity RANS or LES could be used.

## 4 CONCLUSIONS

A QS method for the prediction of the unsteady thrust of a propeller has been quantitatively validated against experimental results, with higher accuracy results found for the lower EAR propeller. The QS method is shown to be versatile with the incorporation of modelling extensions demonstrated. It is essential to know to what extent the QS method can be correctly extended so that it may be applied as a design tool in different nominal wakes. Areas of weakness were identified and where possible corrected and caveats on the application of the QS method were defined.

## REFERENCES

Blake, W. K. 2017. Mechanics of flow-induced sound and vibration, Volume 2: Complex flow-structure interactions, Academic press.

Boswell, R. J. & Miller, M. L. 1968. Unsteady propeller loading-measurement, correlation with theory, and parametric study. David Taylor Research Center, Report 2625.

Breslin, J. P. 1971 Exciting-Force Operators for Ship Propellers. *Journal of Hydronautics*, *5*(3), pp.85-90.

Breslin, J. P. 1970. Theoretical and experimental techniques for practical estimation of propeller-induced vibratory forces. *Transactions of the Society of Naval Architects and Marine Engineers,* 78**,** 23-40.

Breslin, J. P. 1992. An analytical theory of propeller-generated effective wake. *In:* WICKHAM, P. (ed.) *Wave Asymptotics.* Cambridge University Press.

Breslin, J. P. & Andersen, P. 1996. *Hydrodynamics of ship propellers*. Cambridge University Press.

Carlton, J. 2012. *Marine propellers and propulsion*. Butterworth-Heinemann, 3rd Edition.

Denny, S. B. 1968. Cavitation and open water performance tests of a series of propellers designed by lifting-surface methods. David Taylor Research Center, Report 2878.

Glegg, S. & W. Devenport 2017. Aeroacoustics of low Mach number flows: fundamentals, analysis, and measurement, Academic Press.

Jessup, S. D. 1990. Measurement of multiple blade rate unsteady propeller forces. David Taylor Research Center, Report DTRC-90/015.

Jin, Y., Dylejko, P., Skvortsov. A. & Duffy, J. 2018 Prediction of unsteady propeller performance in an inhomogeneous wake. Proceedings of ACOUSTICS 2018, 7-9 November, Adelaide, Australia

Kazarina, M. & Golubev, V. V. 2019 On 3D effects in Gust-Airfoil and Turbulence-Airfoil Interaction Responses AIAA Scitech 2019 Forum.

Kerwin, J. E. 1976. A deformed wake model for marine propelleors. David Taylor Research Center.

Kerwin, J. E. 1986. Marine propellers. *Annual review of fluid mechanics*, *18*(1), 367-403.

Maljaars, P., Kaminski, M. & den Besten, H., 2018. Boundary element modelling aspects for the hydro-elastic analysis of flexible marine propellers. *Journal of Marine Science and Engineering*, *6*(2) p.67.

McCarthy, J. H. 1961. On the calculation of thrust and torque fluctuations of propellers in nonuniform wake flow. David Taylor Model Basin, Report 1533.

Mugridge, B.D., 1970. Sound radiation from aerofoils in turbulent flow. *Journal of Sound Vibration*, *13*, p.362.

Roddy, R. F. 2011. A fast quasi-steady procedure for estimating the unsteady forces and moments on a marine propeller behind a hull. *Proceedings of the Second International Symposium on Marine Propulsors*.

Sasajima, T. 1978. Usefulness of quasi-steady approach for estimation of propeller bearing forces. *Propellers '78 Symposium.* Virginia Beach, Virginia.

Schwanecke, H. 1975 Comparative Calculation on Unsteady Propeller Blade Forces. In *Report of Propeller Committee, Fourteenth International Towing Tank Conference*.

Smith, D.R. & Slater, J.E. 1988 *The geometry of marine propellers* (No. DREA-TM-88/214). Defence Research Establishment Atlantic, Dartmouth, Nova Scotia.

Tanibayashi, J. 1980. Practical Approach to Unsteady Problems of Marine Propellers by Quasi-Steady Method of Calculation. Mitsubishi Technical Bulletin No. 143.

Valentine, D. T., & Kader, R. D. 1976 *Experimental Investigation of the Effect of Propeller Blade Pitch on Propeller-Produced Unsteady Bearing Forces and Moments*. David Taylor Research Center, 76-0137.